Original Article

The correlation between contrast-enhanced ultrasound Liver Imaging Reporting and Data System classification and differentiation grades of combined hepatocellular carcinoma-cholangiocarcinoma

Jingwen Yang^, Jiazhi Cao^, Xiaomiao Ruan^, Youxiang Ren^, Wenwu Ling^

Department of Medical Ultrasound, West China Hospital of Sichuan University, Chengdu, China

Contributions: (I) Conception and design: W Ling, J Yang; (II) Administrative support: W Ling; (III) Provision of study materials or patients: W Ling; (IV) Collection and assembly of data: J Yang, X Ruan, J Cao; (V) Data analysis and interpretation: J Yang, Y Ren; (VI) Manuscript writing: All authors; (VII) Final approval of manuscript: All authors.

Correspondence to: Wenwu Ling, PhD. Department of Medical Ultrasound, West China Hospital of Sichuan University, No. 37 Guoxuexiang, Chengdu 610041, China. Email: lingwenwubing@163.com.

Background: The contrast-enhanced ultrasound (CEUS) Liver Imaging Reporting and Data System (LI-RADS) classification offers a framework for risk stratification in evaluating liver lesions in patients at risk for hepatocellular carcinoma (HCC). However, its clinical utility in combined HCC-cholangiocarcinoma (cHCC-CCA) has been less extensively studied. The degree of tumor differentiation is clinically significant in determining prognosis, making the analysis of imaging features across different differentiation levels essential. Additionally, studies indicate a correlation between the proportion of HCC and intrahepatic cholangiocarcinoma (ICC) components in cHCC-CCA lesions and their corresponding imaging characteristics. Therefore, the aim of this study was to assess the association of CEUS LI-RADS with the histopathological components and degree of differentiation in cHCC-CCA.

Methods: Medical records and CEUS images of patients with cHCC-CCA pathologically confirmed between April 2020 and April 2023 were reviewed. The predominance and degree of differentiation of HCC and ICC components in cHCC-CCA were analyzed via histopathological examination. The chi-square test and two-tailed Student *t*-test were employed to compare differences in general clinical characteristics, ultrasound features, and LI-RADS classification across various levels of differentiation and pathological components.

Results: A total of 47 patients with cHCC-CCA were included in this study, comprising 39 men and 8 women, with a mean age of 56.2±8.5 years. A total of 47 lesions were analyzed. These lesions were classified according to the degree of differentiation from lower to higher as follows: poorly differentiated in 20 lesions (42.6%), moderately-poorly differentiated in 17 lesions (36.2%), and moderately differentiated in 10 lesions (21.3%). The CEUS features of lesions with varying degrees of differentiation were analyzed. It was observed that lower degrees of differentiation were associated with more pronounced early washout (P=0.028) and an increased likelihood of being classified as LR-M category under the CEUS LI-RADS classification system (P=0.043). Based on the predominance of pathological components, 36 lesions were pathologically confirmed as HCC predominant, and 11 lesions were confirmed as ICC predominant. Their ultrasound characteristics were analyzed, revealing that ICC-predominant cHCC-CCA lesions were more likely to exhibit regular

^ ORCID: Jingwen Yang, 0009-0004-9172-3577; Jiazhi Cao, 0009-0001-7628-6872; Xiaomiao Ruan, 0000-0002-8658-0100; Youxiang Ren, 0009-0005-8420-1559; Wenwu Ling, 0000-0002-6449-3831.

shape (P=0.013) and well defined margins (P=0.010) and have an early onset of washout (P=0.023). However, the CEUS LI-RADS classification was not effective in distinguishing the predominance of the pathological cHCC-CCA components (P=0.283).

Conclusions: cHCC-CCAs classified as LR-M based on CEUS LI-RADS tend to be poorly differentiated, but the dominant pathologic component could be either HCC or ICC. cHCC-CCA lesions with ICC predominance were associated with early washout, whereas HCC-predominant lesions were associated with late washout. Additionally, the margins of HCC-predominant lesions were more ill-defined and irregular in shape compared to those of ICC-predominant lesions.

Keywords: Combined hepatocellular carcinoma-cholangiocarcinoma (cHCC-CCA); ultrasonography; Liver Imaging Reporting and Data System (LI-RADS); histopathological components and differentiation

Submitted Jul 20, 2024. Accepted for publication Oct 25, 2024. Published online Dec 23, 2024.
doi: 10.21037/qims-24-1483
View this article at: https://dx.doi.org/10.21037/qims-24-1483

Introduction

Combined hepatocellular carcinoma-cholangiocarcinoma (cHCC-CCA) is a rare subtype of primary liver cancer that encompasses both hepatocellular carcinoma (HCC) and intrahepatic cholangiocarcinoma (ICC) components. In 2019, the World Health Organization classified cHCC-CCA as a tumor exhibiting both HCC and ICC differentiation based on routine hematoxylin and eosin (HE) staining in histopathological examinations (1). Patients with cHCC-CCA exhibit demographic characteristics and clinical features that overlap with those of HCC and ICC, complicating differential diagnosis. The prognosis for cHCC-CCA is typically poor due to its biological behavior, which is more aggressive than that of isolated HCC (2,3).

The imaging characteristics of cHCC-CCA frequently overlap with those of HCC and ICC, thereby complicating the diagnostic process (4). Studies have demonstrated that the majority of cHCC-CCA tumors exhibit imaging characteristics similar to ICC. This observation has been corroborated by studies using the Liver Imaging Reporting and Data System (LI-RADS) term target-like appearance (5,6). Multiphase computed tomography (CT) and magnetic resonance imaging (MRI) can significantly aid in the diagnosis of cHCC-CCA (7,8). However, the preoperative diagnosis of cHCC-CCA remains challenging due to the histomorphological and functional heterogeneity arising due to variability in tumor component proportions, often resulting in the misdiagnosis of cHCC-CCA as HCC or ICC (9). Contrast-enhanced ultrasound (CEUS) plays a pivotal role in the diagnosis, treatment, and follow-up of patients with liver diseases due to its convenience and capability for real-time dynamic imaging. The American College of Radiology (ACR) LI-RADS is a recently developed framework designed to standardize the interpretation, reporting, and collection of CEUS, CT, and MRI data of patients at risk for HCC (10,11). However, the diagnostic efficacy of CEUS LI-RADS for cHCC-CCA remains unclear due to a lack of comprehensive studies. Previous research indicates that the enhancement pattern observed in CEUS for cHCC-CCA is influenced by the relative proportions of HCC and ICC components. Additionally, this pattern displays characteristics that vary depending on the size of the lesion (12). A few studies have managed to elucidate the differences and associations related to cHCC-CCA with varying degrees of differentiation in terms of CEUS LI-RADS and clinical features. The degree of tumor differentiation is related to prognosis, and thus analyzing the imaging features of different differentiation levels is clinically relevant. It has also been demonstrated that the proportion of HCC and ICC components in cHCC-CCA lesions correlates with their imaging characteristics; furthermore, patients with a higher percentage of HCC components in their lesions exhibit longer disease-free survival (13). Therefore, the composition of HCC and ICC in cHCC-CCA lesions may also be associated with patient prognosis.

The aim of this study was to retrospectively analyze the clinical characteristics of patients with cHCC-CCA with varying degrees of differentiation and pathological components and to investigate the association of CEUS LI-RADS classification with the histological differentiation grade and components of cHCC-CCA. We present

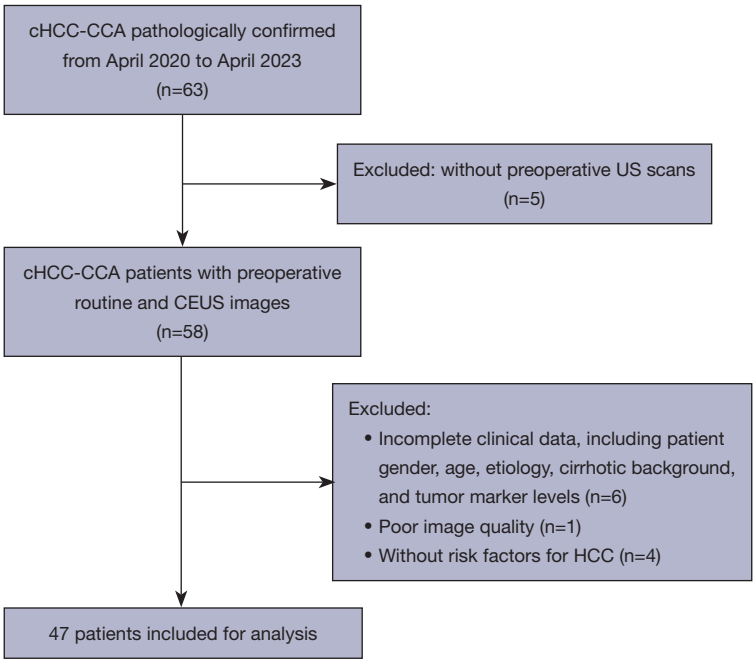

Figure 1 Flowchart of patient inclusion. cHCC-CCA, combined hepatocellular carcinoma-cholangiocarcinoma; US, ultrasound; CEUS, contrast-enhanced ultrasound; HCC, hepatocellular carcinoma.

this article in accordance with the STROBE reporting checklist (available at https://qims.amegroups.com/article/view/10.21037/qims-24-1483/rc).

Methods

Patients

Patients with cHCC-CCA admitted to the Department of Medical Ultrasound at West China Hospital of Sichuan University, from April 2020 to April 2023, and who met the specified inclusion and exclusion criteria were retrospectively analyzed. A flow diagram for the study population is presented in *Figure 1*. A total of 47 patients (47 lesions) were ultimately included in the study. This study was conducted in accordance with the Declaration of Helsinki (as revised in 2013) and was approved by the Ethics Committee of West China Hospital, Sichuan University (No. 1398). The requirement for individual consent was waived due to the retrospective nature of the analysis.

Ultrasound scans

Ultrasonography was conducted using a diagnostic machine equipped with either a C5-1 or L9-3 probe (Mindray, Shenzhen, China). Contrast-specific pulse inversion harmonic imaging, with a mechanical index of less than 0.1, was employed for all CEUS examinations according to the technical guidelines of the World Federation of Ultrasound in Medicine and Biology and the European Federation of Societies of Ultrasound in Medicine and Biology (WFUMB-EFSUMB) (14). A 20-gauge catheter was inserted into the antecubital vein, and the ultrasound contrast agent (SonoVue, Bracco, Milan, Italy) was administered in doses of 1.2 to 2.4 mL, followed by a 5-mL flush with 0.9% NaCl solution. The imaging timer was initiated simultaneously with the injection of the SonoVue contrast agent. The region of interest, encompassing the target hepatic nodule and surrounding hepatic parenchyma, was imaged continuously for the first 60 seconds and then intermittently until the washout or disappearance of hepatic parenchymal enhancement was observed with confidence, typically at 5 minutes or after. The arterial, portal, and late phases were defined as 10–30, 31–120, and 121–300 seconds post-injection, respectively, in accordance with the WFUMB-EFSUMB technical recommendations (14).

All patients underwent routine liver ultrasound scanning. For patients with multiple lesions, the largest lesion was selected as the observation target. Each target lesion was

evaluated across all time phases, with the pertinent image characteristics being documented. Real-time CEUS videos or CEUS images from different time phases were stored for subsequent image analysis.

Image analysis and CEUS LI-RADS classification

During routine ultrasound examination, the size, echo intensity, margins, and morphology of the lesions were meticulously recorded. Round and oval shapes were designated as regular forms, whereas all other shapes were classified as irregular. Based on the degree of enhancement of the lesion in the arterial phase compared with the surrounding liver parenchyma, three primary CEUS features were assessed: homogeneous arterial phase hyperenhancement (APHE), rim APHE, and heterogeneous APHE. According to the 2017 version of the CEUS LI-RADS (10), early washout was defined as that commencing within 60 seconds of contrast agent injection, while late washout was defined as that commencing at or beyond 60 seconds. Washout that appeared black or punched out within 2 minutes of contrast agent injection was categorized as marked washout, whereas all other washouts were classified as mild. In accordance with the 2017 edition of the ACR LI-RADS, the LR-M (malignancy) on CEUS was defined by the presence of any one of the following three criteria: rim APHE, early washout, or marked washout. The criteria for the LR-5 (definitely HCC) category included lesions measuring ≥10 mm, non-rim APHE, and the presence of late or mild washout. The criterion for LR-TIV (tumor in vein) was the presence of enhanced soft tissue within a vein.

All images were independently and randomly analyzed by two physicians, each with over 5 years of experience in liver CEUS examinations. The enhancement patterns and characteristics in the arterial, portal, and late phases were documented. In cases of disagreement, a senior physician with more than 10 years of experience in hepatic CEUS examinations re-evaluated the images and provided the final decision.

Histopathology analysis

Pathological information was obtained through surgical resection in 43 patients and confirmed by preoperative biopsy in four patients. The degree of pathological differentiation of cHCC-CCA lesions is determined by the differentiation status of the carcinoma cells constituting the major component. These are classified as poorly differentiated, moderately poorly differentiated, moderately differentiated, moderately highly differentiated, and highly differentiated. Surgical specimens of liver tumors and the surrounding liver tissue were fixed in 10% formalin, routinely paraffin-embedded, and then subjected to tissue sectioning and HE staining. cHCC-CCA lesions comprise two pathological types of cancer cells: HCC predominant or ICC predominant. HCC-predominant lesions contain more than 50% HCC content, whereas ICC-predominant lesions contain more than 50% ICC content.

Two physicians, each with over 8 years of experience in diagnostic liver pathology, independently evaluated and diagnosed the specimens, including the tumor type and degree of pathological differentiation. In cases of discrepancy, a third physician with more than 15 years of experience in liver pathology re-evaluated the slides and provided the final diagnosis.

Statistical analysis

A P value <0.05 was considered statistically significant. Statistical analyses were performed using SPSS 26 software (IBM Corp., Armonk, NY, USA). Numerical data are presented as the mean ± standard deviation. Continuous variables were compared using the two-tailed Student *t*-test, while categorical variables were compared using the Chi-squared test or the Mann-Whitney test. Interobserver agreement among the readers for CEUS LI-RADS categories was assessed using the kappa statistic. A kappa value between 0.81 and 1 was considered indicative of almost perfect agreement, 0.61 to 0.80 substantial agreement, 0.41 to 0.60 moderate agreement, 0.21 to 0.40 fair agreement, and 0.01 to 0.20 poor agreement (15).

Results

Patient characteristics

In this study, patients (39 men and 8 women; average age 56.2±8.5 years; age range 40 to 70 years), each with a single lesion, were ultimately included. Among these patients, 44 (93.6%) had chronic hepatitis B (CHB), and 3 (6.4%) had chronic hepatitis C (CHC). Cirrhosis was present in 26 (55.3%) patients. In addition, tumor marker tests showed elevated alpha-fetoprotein (AFP) levels (16) in 24 (51.1%) patients, elevated carcinoembryonic antigen (CEA) levels in 8 (17.0%) patients, elevated carbohydrate antigen 19-9

Table 1 General clinical characteristics of 47 patients with cHCC-CCA stratified by different degrees of pathological differentiation and pathological components

Clinical characteristics	Pathological differentiation				Pathological components		
	Poor differentiation (n=20)	Moderate-poor differentiation (n=17)	Moderate differentiation (n=10)	P value	HCC predominant (n=36)	ICC predominant (n=11)	P value
Gender (M/F)	15/5	15/2	9/1	0.453	32/4	7/4	0.051
Age (years)	55.6±9.0	56.9±7.3	56.2±10.0	0.904	56.5±8.5	55.2±8.8	0.657
Etiology							
CHB/CHC	19/1	16/1	9/1	0.865	34/2	10/1	0.675
AFP (≥20/<20 ng/mL)	9/11	8/9	7/3	0.399	20/16	4/7	0.265
CEA (≥5/<5 ng/mL)	1/19	5/12	2/8	0.138	6/30	2/9	0.907
CA19-9 (≥30/<30 U/mL)	5/15	6/11	5/5	0.392	13/23	3/8	0.588
CA125 (≥24/<24 U/mL)	4/16	3/14	4/6	0.372	9/27	2/9	0.640
Cirrhosis (yes/no)	8/12	13/4	5/5	0.078	20/16	6/5	0.953

Data are presented as number or mean ± SD. cHCC-CCA, combined hepatocellular carcinoma-cholangiocarcinoma; HCC, hepatocellular carcinoma; ICC, intrahepatic cholangiocarcinoma; M, male; F, female; CHB, chronic hepatitis B; CHC, chronic hepatitis C; AFP, alpha-fetoprotein; CEA, carcinoembryonic antigen; CA19-9, carbohydrate antigen 19-9; CA125, cancer antigen 125; SD, standard deviation.

(CA19-9) levels in 16 (34.0%) patients, and elevated cancer antigen 125 (CA125) levels in 11 (23.4%) patients.

Pathological analysis of these lesions revealed the following distribution according to the degree of differentiation: 20 lesions (42.6%) were classified as poorly differentiated, 17 lesions (36.2%) as moderately poorly differentiated, and 10 lesions (21.3%) as moderately differentiated. Notably, there were no lesions classified as moderately highly differentiated or hyperdifferentiated. Among the 47 lesions, HCC predominated in 36 cases (76.6%), while ICC predominated in 11 cases (23.4%). The lesions were categorized based on the degree of pathological differentiation and pathological components. Subsequently, the clinical data of patients within each group were statistically analyzed. The results indicated no significant differences in the general data of patients with varying degrees of pathological differentiation and different pathological components, as presented in *Table 1*.

Imaging features and the CEUS LI-RADS classification

The mean diameters of the nodules in poorly differentiated, moderately poorly differentiated, and moderately differentiated lesions were 4.9±2.5, 4.3±2.9, and 5.4±3.7 cm, respectively, as shown in *Table 2*; in these three groups of lesions, the echogenicity predominantly displayed hypoechoic characteristics, with proportions of 85.0% (17/20), 88.2% (15/17), and 70.0% (7/10), respectively. Additionally, most lesions presented with poorly defined margins and irregular shapes. In the poorly differentiated, moderately poorly differentiated, and moderately differentiated lesions, indistinct margins were observed in 60.0% (12/20), 70.6% (12/17), and 80.0% (8/10) of cases, respectively, while irregular shapes were noted in 60.0% (12/20), 52.9% (9/17), and 70.0% (7/10) of cases, respectively.

In CEUS, necrosis, as indicated by lesions with perfusion defects, was observed in cHCC-CCA lesions of varying differentiation degrees. Specifically, necrosis was observed in three cases of poorly differentiated lesions, two cases of moderately–poorly differentiated lesions, and two cases of moderately differentiated lesions. Additionally, all lesions exhibited hyperenhancement during the arterial phase (APHE). Among the poorly differentiated lesions, 55.0% (11/20) presented with homogeneous APHE, 40.0% (8/20) with rim APHE, and 5.0% (1/20) with heterogeneous APHE. Among the moderately-poorly differentiated lesions, 52.9% (9/17) presented with homogeneous APHE, 23.5% (4/17) with exhibited rim APHE, and 23.5% (4/17) with heterogeneous APHE. Furthermore, washout was observed in all lesions. Across the three types of lesions, the majority exhibited marked washout, with 60.0% (12/20), 58.8% (10/17), and 30.0% (3/10) observed in

Table 2 CEUS features of cHCC-CCA lesions with different degrees of pathological differentiation and pathological components

Imaging features	Pathological differentiation				Pathological components		
	Poor differentiation (n=20)	Moderate-poor differentiation (n=17)	Moderate differentiation (n=10)	P value	HCC predominant (n=36)	ICC predominant (n=11)	P value
Nodule size (cm)	4.9±2.5	4.3±2.9	5.4±3.7	0.359	5.0±3.1	4.1±1.9	0.367
Echogenicity				0.453			0.424
Hypoechoic	17 (85.0)	15 (88.2)	7 (70.0)		29 (80.6)	10 (90.9)	
Hyperechoic	3 (15.0)	2 (11.8)	3 (30.0)		7 (19.4)	1 (9.1)	
Ill-defined margins	12 (60.0)	12 (70.6)	8 (80.0)	0.521	28 (77.7)	4 (36.3)	0.010*
Irregular shape	12 (60.0)	9 (52.9)	7 (70.0)	0.683	25 (69.4)	3 (27.3)	0.013*
Necrosis on CEUS	3 (15.0)	2 (11.8)	2 (20.0)	0.845	6 (16.7)	1 (9.1)	0.537
Enhancement pattern				0.284			0.239
Homogeneous APHE	11 (55.0)	9 (52.9)	7 (70.0)		23 (63.9)	4 (36.4)	
Rim APHE	8 (40.0)	4 (23.5)	1 (10.0)		8 (22.2)	5 (45.5)	
Heterogeneous APHE	1 (5.0)	4 (23.5)	2 (20.0)		5 (13.9)	2 (18.2)	
Timing of washout onset				0.028*			0.023*
Early (<60 s)	16 (80.0)	10 (58.8)	3 (30.0)		19 (52.8)	10 (90.9)	
Late (≥60 s)	4 (20.0)	7 (41.2)	7 (70.0)		17 (47.2)	1 (9.1)	
Degree of washout				0.253			0.918
Marked (as observed within first 120 s)	12 (60.0)	10 (58.8)	3 (30.0)		19 (52.8)	6 (54.5)	
Mild	8 (40.0)	7 (41.2)	7 (70.0)		17 (47.2)	5 (45.5)	
CEUS LI-RADS category				0.043*			0.283
LR-5	2 (10.0)	5 (29.4)	6 (60.0)		12 (33.3)	1 (9.1)	
LR-M	17 (85.0)	10 (58.8)	3 (30.0)		21 (58.3)	9 (81.8)	
LR-TIV	1 (5.0)	2 (11.8)	1 (10.0)		3 (8.3)	1 (9.1)	
Pathological components				0.954			–
HCC-predominant	15 (75.0)	13 (76.5)	8 (80.0)		–	–	
ICC-predominant	5 (25.0)	4 (23.5)	2 (20.0)		–	–	

Data are presented as mean ± SD or n (%). *, indicates a statistically significant difference with P<0.05. CEUS, contrast-enhanced ultrasound; cHCC-CCA, combined hepatocellular carcinoma-cholangiocarcinoma; HCC, hepatocellular carcinoma; ICC, intrahepatic cholangiocarcinoma; APHE, arterial phase hyperenhancement; LI-RADS, Liver Imaging Report and Data System; SD, standard deviation.

poorly differentiated, moderately-poorly differentiated, and moderately differentiated lesions, respectively; however, there was a decline in the percentage of lesions exhibiting early washout as the degree of differentiation increased, specifically to 80.0% (16/20), 58.8% (10/17), and 30.0% (3/10), respectively (P=0.028).

Portal vein thrombosis was observed in one case of a poorly differentiated lesion, two cases of moderately poorly differentiated lesions, and one case of moderately differentiated lesions, corresponding to the CEUS LI-RADS LR-TIV classification in 5.0% (1/20), 11.8% (2/17), and 10.0% (1/10) of lesions, respectively. With

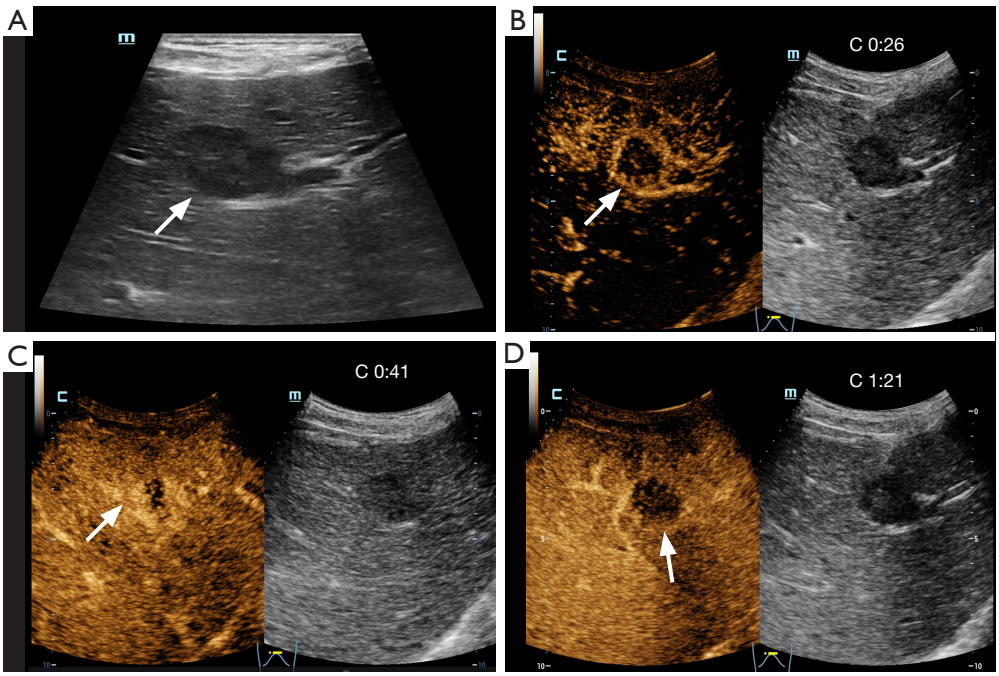

Figure 2 An LR-M lesion in a 58-year-old male patient with CHB. (A) A routine gray-scale ultrasound scan detected a 3.0 cm × 2.1 cm hypoechoic lesion in the left inner lobe of the liver, characterized by well-defined margins and regular shape (arrow). (B) The lesion exhibited rim hyperenhancement in the arterial phase of CEUS (arrow). (C) The lesion demonstrated hyperenhancement 41 seconds after contrast injection (arrow). (D) Marked washout (arrow) in the portal phase. The lesion was classified as LR-M, and pathological examination confirmed that it predominantly consisted of ICC, which was poorly differentiated. C, contrast timer; CHB, chronic hepatitis B; CEUS, contrast-enhanced ultrasound; ICC, intrahepatic cholangiocarcinoma.

the increasing differentiation of lesions, from poorly differentiated moderately–poorly differentiated, to moderately differentiated, the proportions of cHCC-CCA lesions classified as LR-5 by CEUS LI-RADS increased to 10.0% (2/20), 29.4% (5/17), and 60.0% (6/10), respectively, while the proportions classified as LR-M decreased to 85.0% (17/20), 58.8% (10/17), and 30.0% (3/10), respectively, (P=0.043).

Based on the pathological components, the mean diameters of HCC-predominant and ICC-predominant lesions were 5.0±3.1 and 4.1±1.9 cm, respectively, as shown in *Table 2*. In both types of lesions, hypoechoicity was observed in 29 of the HCC-predominant lesions and in 10 of the ICC-predominant lesions. Additionally, 28 HCC-predominant lesions and four ICC-predominant lesions exhibited ill-defined margins (P=0.010). An irregular shape was observed in 69.4% (25/36) of HCC-predominant lesions, whereas only 27.3% (3/11) of ICC-predominant lesions exhibited an irregular shape (P=0.013).

In the CEUS findings, necrosis was identified in six of the HCC-predominant lesions and in one of the ICC-predominant lesions. Among the HCC-predominant lesions, 21 lesions were classified as LR-M based on the presence of at least one of the related CEUS LI-RADS criteria (version 2017), which showed the following distribution: rim-like APHE in eight lesions, early washout in 19 lesions, and marked washout in 19 lesions. Among the ICC-predominant lesions, nine were classified as LR-M (*Figure 2*) and one as LR-TIV. Rim-like APHE was observed in five lesions, early washout in 10, marked washout in six, and portal vein thrombus enhancement in one. Homogeneous or heterogeneous APHE exceeding 10 mm in diameter, along with mild and late washout, was observed in 12 HCC-predominant lesions and one ICC-predominant lesion, and these were categorized as LR-5 (*Figure 3*).

Interobserver agreement

The interobserver agreement for CEUS features and CEUS

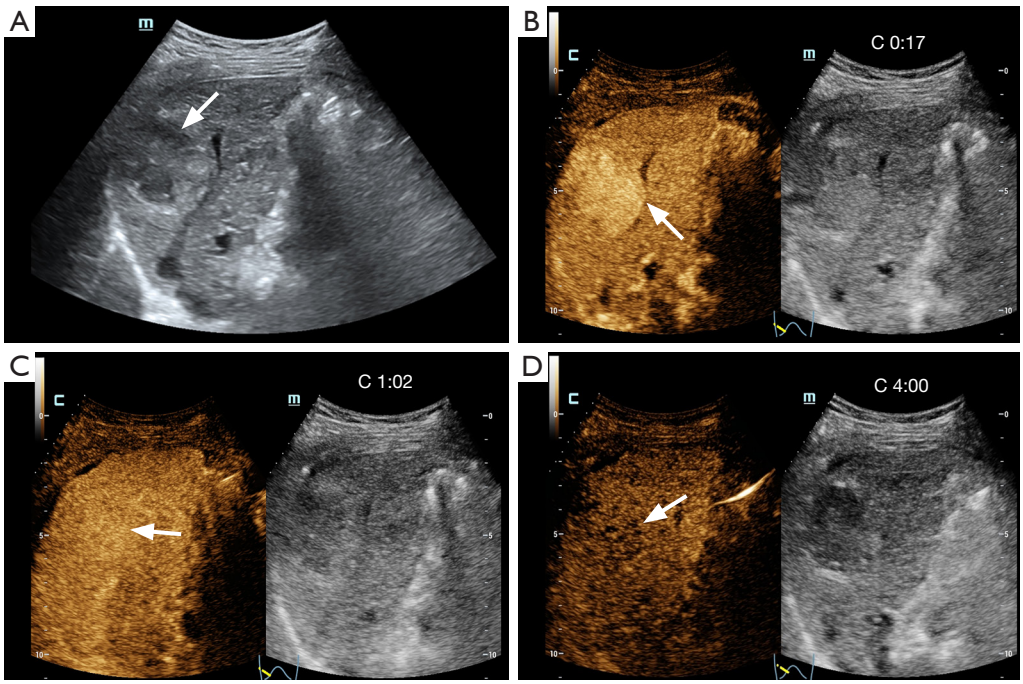

Figure 3 An LR-5 lesion in a 52-year-old male patient with CHB. (A) A heterogeneous hypoechoic lesion measuring 4.5 cm × 4.0 cm, with ill-defined margins and irregular shape, was detected in the upper segment of the right liver lobe on gray-scale ultrasound (arrow). (B) CEUS of the lesion during the arterial phase revealed homogeneous hyperenhancement (arrow). (C) In the portal phase, the lesion exhibited isoenhancement (arrow). (D) The lesion exhibited slightly reduced enhancement in the late phase (arrow). The lesion was classified as LR-5, and pathological examination confirmed that it predominantly consisted of HCC, which was poorly differentiated. Pathological analysis also confirmed the presence of cirrhosis (S4). C, contrast timer; CHB, chronic hepatitis B; CEUS, contrast-enhanced ultrasound; HCC, hepatocellular carcinoma; S4, Scheuer classification for cirrhosis, stage 4.

LI-RADS classification of cHCC-CCA lesions is presented in *Table 3*. The interobserver agreement for arterial phase enhancement features demonstrated good concordance, with a kappa value of 0.622. Furthermore, there was significant interobserver agreement regarding the initiation time and extent of washout, with kappa values of 0.824 and 0.78, respectively. The interobserver agreement for CEUS LI-RADS category was substantial (κ=0.640).

Discussion

cHCC-CCA is a primary liver malignancy characterized by both HCC and ICC differentiation and accounts for fewer than 5% of all primary hepatic tumors (17). Although cHCC-CCA contains both HCC and ICC components, its prognosis is more closely aligned with that of ICC (18,19). The degree of tumor differentiation significantly influences the prognosis and overall survival (20,21). Poorly differentiated tumors typically exhibit progenitor cell characteristics linked to chromosomal instability and *TP53* mutations (20,22-24). In our study, all cHCC-CCA lesions were graded based on pathological findings, with 42.6% of the lesions classified as poorly differentiated. In our cohort, based on the predominance of pathological components, 36 out of 47 cHCC-CCA lesions were HCC predominant, while 11 were ICC predominant. This is consistent with previous studies, which reported that the majority of cHCC-CCA and ICC lesions are poorly differentiated and the enhancement pattern of cHCC-CCA predominantly resembles that of HCC in most cases (2,25,26). Additionally, the imaging resemblance of cHCC-CCA to HCC in the majority of cases may be attributable to the high prevalence of HCC risk factors among the screened patients, potentially introducing a selection bias. The absence of highly differentiated components in the cHCC-CCA lesions may be explained by the differing cellular origins of the lesions (3).

The study characterized and analyzed the clinical

Table 3 The interobserver agreement for CEUS features and CEUS LI-RADS classification in 47 cHCC-CCA lesions

CEUS feature	Reviewer A	Reviewer B	κ
Arterial enhancement pattern			0.622
Homogeneous APHE	28	27	
Rim APHE	13	13	
Heterogeneous APHE	6	7	
Timing of washout onset			0.824
Early (<60 s)	29	27	
Late (≥60 s)	18	20	
Degree of washout			0.785
Marked (as observed within first 120 s)	25	28	
Mild	22	19	
CEUS LI-RADS category			0.640
LR-5	13	16	
LR-M	30	27	
LR-TIV	4	4	

CEUS, contrast-enhanced ultrasound; LI-RADS, Liver Imaging Report and Data System; cHCC-CCA, combined hepatocellular carcinoma-cholangiocarcinoma; APHE, arterial phase hyperenhancement.

features of patients with cHCC-CCA with varying degrees of differentiation and pathological components. cHCC-CCA is more commonly observed in male patients (27); however, the specific degree of differentiation and pathological components in our study was not associated with gender (P=0.382). Additionally, age, etiology, and the presence of a cirrhotic background in patients with cHCC-CCA were not correlated with the degree of differentiation and pathological components. Previous reports suggest that the simultaneous elevation of AFP and CA19-9 may indicate a possible diagnosis of cHCC-CCA (28). However, in this study, there were no significant differences in serum tumor marker levels of AFP, CEA, CA19-9, or CA125 among the patients with cHCC-CCA with varying degrees of differentiation and pathological components. An analysis of routine ultrasound findings revealed that ICC-predominant lesions were more likely to present with well-defined margins and regular shapes, whereas HCC-predominant lesions exhibited a higher probability of presenting with blurred margins and irregular shapes, which is consistent with previous research (26).

The CEUS LI-RADS was established to provide standardized imaging information for the screening and monitoring of HCC (29). In contrast, the LR-M category was defined to indicate lesions with a high probability of malignancy and is not specific to HCC (10). Nonetheless, the LR-M category demonstrates diagnostic value for both HCC and non-HCC liver malignancies (30,31). The imaging presentation and pathological findings of cHCC-CCA were consistent, with features and major components from both tumor types (32). However, classifying the lesions into HCC-predominant and ICC-predominant categories based on the major pathological components of cHCC-CCA revealed that both types predominantly exhibited the LI-RADS classification of LR-M. Specifically, 58.3% of HCC-predominant lesions and 81.8% of ICC-predominant lesions were categorized as LR-M (P=0.283). Regarding washout time, 90.9% of ICC-predominant lesions exhibited early washout, whereas only 52.8% of HCC-predominant lesions did so (P=0.023). The results indicate a correlation between washout time and pathological composition: early washout suggests that ICC is the predominant component in cHCC-CCA, whereas late washout suggests that HCC is the predominant component. Other studies have reported similar findings, indicating that the enhancement pattern of CEUS in cHCC-CCA is dependent on the relative proportions of HCC and ICC components (12). The

inability of CEUS LI-RADS to effectively differentiate the major pathological components of cHCC-CCA may be attributed to the fact that the LR-M category does not exclude HCC. Consequently, even HCC-predominant lesions tend to be classified as LR-M within the LI-RADS framework due to the coexistence of ICC pathological components. This classification is an expected outcome of the higher diagnostic sensitivity of the CEUS LR-M category for non-HCC malignancies.

Imaging descriptions of the cHCC-CCA subtype have been infrequently reported compared to those of HCC and ICC. In this study, the 47 cHCC-CCA lesions included were classified as poorly differentiated, moderately–poorly differentiated, and moderately differentiated based on the degree of differentiation. Their clinical and ultrasonographic features were characterized, and the association between the CEUS LI-RADS classification and the degree of differentiation of cHCC-CCA was determined. The results demonstrated that as the degree of differentiation of cHCC-CCA lesions increased, the greater the likelihood was of a CEUS LI-RADS LR-5 classification. Conversely, as the degree of differentiation decreased, the greater the likelihood was of an LR-M classification (P=0.043). Among all CEUS features, early washout was the predominant characteristic leading to the classification of LR-M (P=0.028). In CEUS, malignant lesions typically exhibit a tendency to wash out. Although the precise mechanisms underlying this phenomenon are not entirely understood, it can be partially attributed to the comparatively low blood volume of these tumors relative to the surrounding liver tissue (33). Poorly differentiated tumors are frequently associated with disorganized vascular structures, characterized by abnormal branching and neovascularization (34). However, previous studies have indicated that the vascular distribution in poorly differentiated HCC tends to be reduced both radiologically and pathologically (35,36). This is consistent with our findings, with poorly differentiated cHCC-CCA lesions being characterized by early washout, which is attributable to their lower blood supply and reduced blood volume.

This study demonstrated that cHCC-CCA lesions were more likely to be categorized as CEUS LI-RADS LR-5 as the degree of differentiation increased, while a lower degree of differentiation tended to correspond to the LR-M category. Thus, CEUS LI-RADS may serve as a valuable noninvasive predictive tool for the clinical management of patients with cHCC-CCA and thus enhance diagnostic accuracy.

The limitations of this study include its retrospective nature, limited sample size, the gender discrepancy within the patient cohort, and the absence of a control group of HCC or ICC for comparison. Further prospective studies are needed to validate these findings. Moreover, the parameters selected for CEUS were qualitative rather than quantitative. However, due to the low prevalence of cHCC-CCA and the unavailability of biopsies for all lesions in patients, this limitation was challenging to overcome. Future research could focus on multicenter validation studies and examine the integration of CEUS LI-RADS with other imaging techniques and biomarkers to improve the diagnosis of cHCC-CCA.

Conclusions

There was a significant association between CEUS LI-RADS and the differentiation of cHCC-CCA, suggesting its potential value in the noninvasive assessment of tumor differentiation. cHCC-CCA lesions with ICC predominance were associated with early washout, whereas HCC-predominant lesions were linked to late washout. Additionally, the margins of HCC-predominant lesions were more likely to be ill-defined and irregular in shape compared to those of ICC-predominant lesions. These findings support the application of CEUS LI-RADS to enhance the diagnostic and prognostic capabilities in the clinical management of cHCC-CCA.

Acknowledgments

Funding: None.

Footnote

Reporting Checklist: The authors have completed the STROBE reporting checklist. Available at https://qims.amegroups.com/article/view/10.21037/qims-24-1483/rc

Conflicts of Interest: All authors have completed the ICMJE uniform disclosure form (available at https://qims.amegroups.com/article/view/10.21037/qims-24-1483/coif). The authors have no conflicts of interest to declare.

Ethical Statement: The authors are accountable for all aspects of the work in ensuring that questions related to the accuracy or integrity of any part of the work are appropriately investigated and resolved. This study was

conducted in accordance with the Declaration of Helsinki (as revised in 2013) and was approved by the Ethics Committee of West China Hospital, Sichuan University (No. 1398). The requirement for individual consent was waived due to the retrospective nature of the analysis.

References

1. Nagtegaal ID, Odze RD, Klimstra D, Paradis V, Rugge M, Schirmacher P, Washington KM, Carneiro F, Cree IA; WHO Classification of Tumours Editorial Board. The 2019 WHO classification of tumours of the digestive system. Histopathology 2020;76:182-8.
2. Ramai D, Ofosu A, Lai JK, Reddy M, Adler DG. Combined Hepatocellular Cholangiocarcinoma: A Population-Based Retrospective Study. Am J Gastroenterol 2019;114:1496-501.
3. Ye L, Schneider JS, Ben Khaled N, Schirmacher P, Seifert C, Frey L, He Y, Geier A, De Toni EN, Zhang C, Reiter FP. Combined Hepatocellular-Cholangiocarcinoma: Biology, Diagnosis, and Management. Liver Cancer 2024;13:6-28.
4. Fowler KJ, Sheybani A, Parker RA 3rd, Doherty S, M Brunt E, Chapman WC, Menias CO. Combined hepatocellular and cholangiocarcinoma (biphenotypic) tumors: imaging features and diagnostic accuracy of contrast-enhanced CT and MRI. AJR Am J Roentgenol 2013;201:332-9.
5. Beaufrère A, Calderaro J, Paradis V. Combined hepatocellular-cholangiocarcinoma: An update. J Hepatol 2021;74:1212-24.
6. Potretzke TA, Tan BR, Doyle MB, Brunt EM, Heiken JP, Fowler KJ. Imaging Features of Biphenotypic Primary Liver Carcinoma (Hepatocholangiocarcinoma) and the Potential to Mimic Hepatocellular Carcinoma: LI-RADS Analysis of CT and MRI Features in 61 Cases. AJR Am J Roentgenol 2016;207:25-31.
7. Lu L, Zhang C, Yu X, Zhang L, Feng Y, Wu Y, Xia J, Chen X, Zhang R, Zhang J, Jia N, Zhang S. The Value of Contrast-Enhanced Magnetic Resonance Imaging Enhancement in the Differential Diagnosis of Hepatocellular Carcinoma and Combined Hepatocellular Cholangiocarcinoma. J Oncol 2022;2022:4691172.
8. Majeed NF, Macey M, Amirfarzan MB, Sharifi S, Wortman JR. MRI features of combined hepatocellular-cholangiocarcinoma. Abdom Radiol (NY) 2024. [Epub ahead of print]. doi: 10.1007/s00261-024-04476-5.
9. Chu KJ, Kawaguchi Y, Wang H, Jiang XQ, Hasegawa K. Update on the Diagnosis and Treatment of Combined Hepatocellular Cholangiocarcinoma. J Clin Transl Hepatol 2024;12:210-7.
10. Chernyak V, Fowler KJ, Kamaya A, Kielar AZ, Elsayes KM, Bashir MR, Kono Y, Do RK, Mitchell DG, Singal AG, Tang A, Sirlin CB. Liver Imaging Reporting and Data System (LI-RADS) Version 2018: Imaging of Hepatocellular Carcinoma in At-Risk Patients. Radiology 2018;289:816-30.
11. Wang H, Cao J, Fan H, Huang J, Zhang H, Ling W. Compared with CT/MRI LI-RADS, whether CEUS LI-RADS is worth popularizing in diagnosis of hepatocellular carcinoma?-a direct head-to-head meta-analysis. Quant Imaging Med Surg 2023;13:4919-32.
12. Ye J, Xie X, Lin Y, Liu B, Wang W, Huang X, Huang G. Imaging features of combined hepatocellular-cholangiocarcinoma on contrast-enhanced ultrasound: correlation with clinicopathological findings. Clin Radiol 2018;73:237-43.
13. Yang J, Huang JY, Chen X, Ling WW, Luo Y, Shi YJ, Liu JB, Lu Q, Lyshchik A. Combined hepatocellular-cholangiocarcinoma: can we use contrast-enhanced ultrasound Liver Imaging Reporting and Data System (LI-RADS) to predict the patient's survival? Eur Radiol 2021;31:6397-405.
14. Claudon M, Dietrich CF, Choi BI, Cosgrove DO, Kudo M, Nolsøe CP, et al. Guidelines and good clinical practice recommendations for contrast enhanced ultrasound (CEUS) in the liver--update 2012: a WFUMB-EFSUMB initiative in cooperation with representatives of AFSUMB, AIUM, ASUM, FLAUS and ICUS. Ultraschall Med 2013;34:11-29.
15. Viera AJ, Garrett JM. Understanding interobserver agreement: the kappa statistic. Fam Med 2005;37:360-3.
16. Ji J, Wang H, Li Y, Zheng L, Yin Y, Zou Z, Zhou F, Zhou W, Shen F, Gao C. Diagnostic Evaluation of Des-Gamma-Carboxy Prothrombin versus α-Fetoprotein for Hepatitis B Virus-Related Hepatocellular Carcinoma

in China: A Large-Scale, Multicentre Study. PLoS One 2016;11:e0153227.
17. Jarnagin WR, Weber S, Tickoo SK, Koea JB, Obiekwe S, Fong Y, DeMatteo RP, Blumgart LH, Klimstra D. Combined hepatocellular and cholangiocarcinoma: demographic, clinical, and prognostic factors. Cancer 2002;94:2040-6.
18. Wakizaka K, Yokoo H, Kamiyama T, Ohira M, Kato K, Fujii Y, Sugiyama K, Okada N, Ohata T, Nagatsu A, Shimada S, Orimo T, Kamachi H, Taketomi A. Clinical and pathological features of combined hepatocellular-cholangiocarcinoma compared with other liver cancers. J Gastroenterol Hepatol 2019;34:1074-80.
19. Chen PD, Chen LJ, Chang YJ, Chang YJ. Long-Term Survival of Combined Hepatocellular-Cholangiocarcinoma: A Nationwide Study. Oncologist 2021;26:e1774-85.
20. Lee JS, Thorgeirsson SS. Genome-scale profiling of gene expression in hepatocellular carcinoma: classification, survival prediction, and identification of therapeutic targets. Gastroenterology 2004;127:S51-5.
21. Cai X, Zhai J, Kaplan DE, Zhang Y, Zhou L, Chen X, Qian G, Zhao Q, Li Y, Gao L, Cong W, Zhu M, Yan Z, Shi L, Wu D, Wei L, Shen F, Wu M. Background progenitor activation is associated with recurrence after hepatectomy of combined hepatocellular-cholangiocarcinoma. Hepatology 2012;56:1804-16.
22. Hoshida Y, Nijman SM, Kobayashi M, Chan JA, Brunet JP, Chiang DY, Villanueva A, Newell P, Ikeda K, Hashimoto M, Watanabe G, Gabriel S, Friedman SL, Kumada H, Llovet JM, Golub TR. Integrative transcriptome analysis reveals common molecular subclasses of human hepatocellular carcinoma. Cancer Res 2009;69:7385-92.
23. Boyault S, Rickman DS, de Reyniès A, Balabaud C, Rebouissou S, Jeannot E, Hérault A, Saric J, Belghiti J, Franco D, Bioulac-Sage P, Laurent-Puig P, Zucman-Rossi J. Transcriptome classification of HCC is related to gene alterations and to new therapeutic targets. Hepatology 2007;45:42-52.
24. Na HY, Kim JH, Kim H, Cho JY, Han HS, Jang ES, Kim JW, Jeong SH, Heo J, Kim JW, Kim JW, Ahn S. Multiregional analysis of combined hepatocellular-cholangiocarcinoma reveals histologic diversity and molecular clonality. Histopathology 2024;84:402-8.
25. Yang Z, Shi G. Survival outcomes of combined hepatocellular-cholangiocarcinoma compared with intrahepatic cholangiocarcinoma: A SEER population-based cohort study. Cancer Med 2022;11:692-704.
26. Wang Y, Yang Q, Li S, Luo R, Mao S, Shen J. Imaging features of combined hepatocellular and cholangiocarcinoma compared with those of hepatocellular carcinoma and intrahepatic cholangiocellular carcinoma in a Chinese population. Clin Radiol 2019;74:407.e1-407.e10.
27. Garancini M, Goffredo P, Pagni F, Romano F, Roman S, Sosa JA, Giardini V. Combined hepatocellular-cholangiocarcinoma: a population-level analysis of an uncommon primary liver tumor. Liver Transpl 2014;20:952-9.
28. Li R, Yang D, Tang CL, Cai P, Ma KS, Ding SY, Zhang XH, Guo DY, Yan XC. Combined hepatocellular carcinoma and cholangiocarcinoma (biphenotypic) tumors: clinical characteristics, imaging features of contrast-enhanced ultrasound and computed tomography. BMC Cancer 2016;16:158.
29. Jin H, Cai Y, Zhang M, Huang L, Bao W, Hu Q, Chen X, Zhou L, Ling W. LI-RADS LR-5 on contrast-enhanced ultrasonography has satisfactory diagnostic specificity for hepatocellular carcinoma: a systematic review and meta-analysis. Quant Imaging Med Surg 2023;13:957-69.
30. Wen R, Lin P, Wu Y, Yin H, Huang W, Guo D, Peng Y, Liu D, He Y, Yang H. Diagnostic value of CEUS LI-RADS and serum tumor markers for combined hepatocellular-cholangiocarcinoma. Eur J Radiol 2022;154:110415.
31. Wen R, Huang F, Lin P, Gao R, Pang J, Wu Y, Yin H, Tang Z, Ma Z, He Y, Yang H. Performance of current versus modified CEUS LI-RADS in the diagnosis of non-hepatocellular carcinoma malignancies. Abdom Radiol (NY) 2023;48:3688-95.
32. Sanada Y, Shiozaki S, Aoki H, Takakura N, Yoshida K, Yamaguchi Y. A clinical study of 11 cases of combined hepatocellular-cholangiocarcinoma Assessment of enhancement patterns on dynamics computed tomography before resection. Hepatol Res 2005;32:185-95.
33. Nguyen SA, Merrill CD, Burrowes DP, Medellin GA, Wilson SR. Hepatocellular Carcinoma in Evolution: Correlation with CEUS LI-RADS. Radiographics 2022;42:1028-42.
34. Calderaro J, Couchy G, Imbeaud S, Amaddeo G, Letouzé E, Blanc JF, Laurent C, Hajji Y, Azoulay D, Bioulac-Sage P, Nault JC, Zucman-Rossi J. Histological subtypes of hepatocellular carcinoma are related to gene mutations and molecular tumour classification. J Hepatol 2017;67:727-38.
35. Asayama Y, Yoshimitsu K, Nishihara Y, Irie H, Aishima

S, Taketomi A, Honda H. Arterial blood supply of hepatocellular carcinoma and histologic grading: radiologic-pathologic correlation. AJR Am J Roentgenol 2008;190:W28-34.
36. Asayama Y, Yoshimitsu K, Irie H, Nishihara Y, Aishima S, Tajima T, Hirakawa M, Ishigami K, Kakihara D, Taketomi A, Honda H. Poorly versus moderately differentiated hepatocellular carcinoma: vascularity assessment by computed tomographic hepatic angiography in correlation with histologically counted number of unpaired arteries. J Comput Assist Tomogr 2007;31:188-92.

Cite this article as: Yang J, Cao J, Ruan X, Ren Y, Ling W. The correlation between contrast-enhanced ultrasound Liver Imaging Reporting and Data System classification and differentiation grades of combined hepatocellular carcinoma-cholangiocarcinoma. Quant Imaging Med Surg 2025;15(1):259-271. doi: 10.21037/qims-24-1483

